

Reactive Plasma Species in the Modification of Wool Fibre

X. J. Dai,^A S. M. Hamberger^A and R. A. Bean^{A,B}

^A Plasma Research Laboratory, Research School of Physical Sciences and Engineering, Australian National University, Canberra, ACT 0200, Australia.

^B Division of Wool Technology, CSIRO, Belmont, Vic. 3216, Australia.

Abstract

Physical and chemical changes to the surface properties of wool fibre caused by exposure to RF generated plasma have been studied. Comparison is made between the changes for a wide range of plasma conditions and of the experimentally measured concentrations of the relevant neutral and charged particle species to elucidate those principally responsible and the likely mechanism. Results show that the measured increase in surface energy (from hydrophobic to hydrophilic) is well correlated with the integrated flux to the fibre of atomic oxygen, regardless of its origin. Charged particles appear to have little effect beyond sputtering, while the role of metastable excited oxygen molecules seems to be not statistically significant. Changes in surface chemistry shown by XPS are consistent with direct interaction of reactive O on the C-C and C-H bonds of the lipid layer which forms the outer (~3 nm thick) layer of the natural fibre. Similar but weaker effects sometimes seen with discharges in argon appear to be due to the presence of oxygen as an impurity.

1. Introduction

Many commercially important wool treatments require the surface of the fibres to be first modified, most commonly by rendering the normally hydrophobic surface hydrophilic using chemical chlorination of the lipid layer (Maclaren and Milligan 1981). However, it has become clear that there is a need to replace chlorination by more environmentally acceptable methods to avoid high energy and water consumption in the process as well as environmental pollution. One very effective alternative is to expose the material to the reactive plasma formed by a low pressure discharge, e.g. in oxygen or air (Rakowski 1989).

Low pressure plasmas formed in various gases are already extensively used to modify surfaces in applications for microelectronics, surface etching, polymer treatment, etc. (Crompton *et al.* 1991; Joubert *et al.* 1989; Chou *et al.* 1992; Zawaideh and Kim 1988; Schram *et al.* 1987). We have been investigating the underlying chemical and physical processes involved in the modification of wool fibre surface caused by its exposure to plasmas formed by RF discharges, mainly in oxygen, in which both charged particles and reactive neutrals are formed. Those of obvious interest are atomic oxygen O(¹S) with about 4.2 eV available energy and metastable (singlet ¹Δ_g) excited molecular oxygen with 0.97 eV. This paper describes controlled laboratory experiments aimed at correlating the observable changes in the surface properties of wool fibre, such as its surface energy and

chemical composition as determined using X-ray photoelectron spectroscopy, with its exposure to the various plasma constituents in order to identify which of those present, for example, oxygen atoms, metastable oxygen molecules, or charged particles play the most important role.

In this study the plasma products, generated in a well-controlled RF excited source, flow onto prepared fabric samples placed in a separate reaction chamber inside which the concentration of the relevant plasma constituents are measured. The properties of the exposed samples are subsequently studied after removal from the chamber to quantify the changes produced. The experimental arrangement is described in Section 2. Section 3 summarises the results of measurements of particle concentrations and changes in the surface energy, chemical composition and physical appearance of the fibres. Although the study has been conducted mainly with oxygen plasmas, other gases (Ar, dry air, and H₂) have also been used to help identify and confirm the processes responsible. The results are discussed and a simple model formulated in Section 4.

2. Experimental Arrangement

(2a) Experimental Apparatus

A schematic diagram of the apparatus and the coordinate system used is shown in Fig. 1. The plasma source consists of a glass cylinder, 150 mm diameter and 300 mm long, mounted vertically above a continuously pumped reaction chamber. The working gas (normally industrial oxygen) is fed in at the top via a flow controller at between 6.0 and 12.0 sccm (standard cubic centimetres/minute) to provide a pressure range in the chamber between 10⁻³ and 10⁻¹ mbar (1 mbar = 0.75 Torr) as measured by a capacitance manometer. An electrode-less discharge is produced by a 13.56 MHz industrial RF generator coupled via a matching network to a close-fitting coil on the glass cylinder. Power to the source is supplied in the range 25 to 300 W either continuously or in single pulses of duration between 0.1 and 10 s.

Plasma products generated in the source diffuse into the cylindrical stainless steel reaction chamber, which is 650 mm long and 320 mm in diameter. This separation of the reaction chamber from the plasma source is significant for industrial application as it allows a high concentration of reactive species without the presence of any high electromagnetic fields at the wool and allows isolation from damaging ultra-violet radiation if necessary. At one end of the chamber a hinged door, fitted with a 250 mm diameter glass viewing window, provides access for samples which are located below the source in the chamber on a stainless steel platform. The samples are normally 140×40 mm pieces of lightweight plain woven wool fabric of 155 gm⁻². A fine wire mesh can be interposed between the plasma source and the reaction chamber in order to reduce the flux of charged particles into the chamber without seriously affecting the flux of neutral particles. Six ports in the other end-plate and one in the base of the chamber provide access for Langmuir probes to measure the spatial profile of the plasma parameters. Two opposing ports in the side of the cylindrical chamber, shown in Fig. 1*b* (a side view of the apparatus), provide optical access, e.g. for vacuum ultra-violet (vuv) absorption measurements. The whole system is evacuated by an oil diffusion pump to a base pressure around 10⁻⁶ mbar.

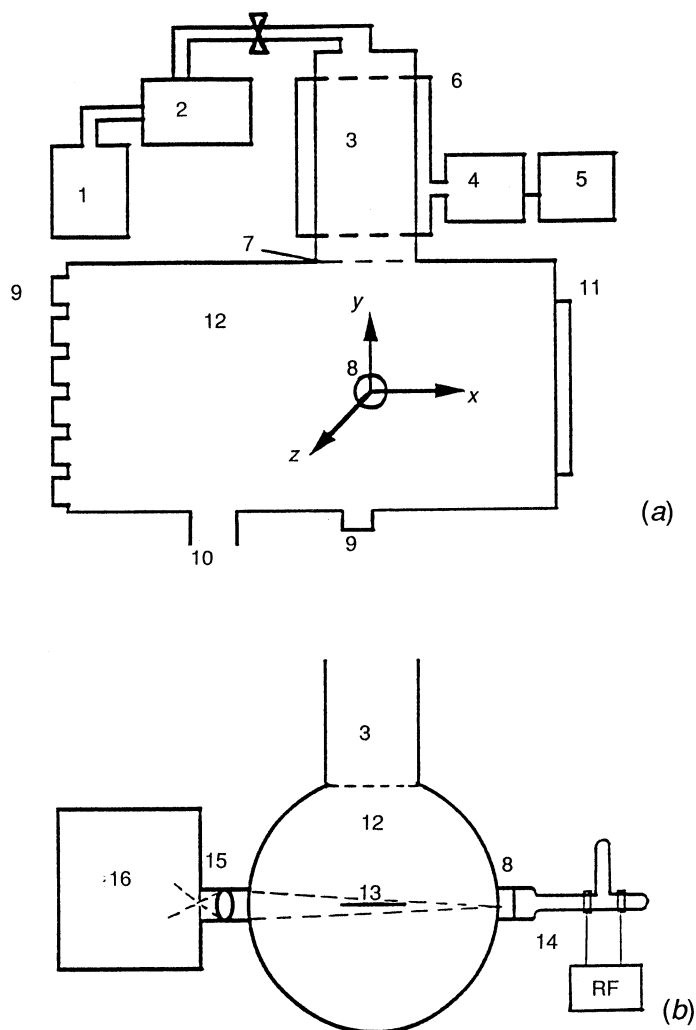


Fig. 1. Schematic diagram of the experimental apparatus. (a) Side-view section: 1, working gas; 2, flow controller; 3, plasma source; 4, RF matching box; 5, RF generator; 6, RF antenna; 7, location of wire mesh when used; 8, MgF_2 window; 9, access ports for Langmuir probes; 10, vacuum system; 11, viewing window and sample access; 12, reaction chamber; 13, sample location; 14, vuv light source; 15, MgF_2 lens; and 16, vuv monochromator and its detection system. (b) End-view section, showing the optical arrangement for vuv absorption measurements.

(2b) Plasma Measurements

A cylindrical Langmuir probe (2.5 mm diameter and 7.0 mm long) is used to measure the plasma parameters. The computer-generated swept bias voltage is supplied via a D/A converter, amplified and applied to the probe. The probe current is measured digitally by the potential drop across a resistor. The probe voltage-current characteristics are analysed numerically to obtain the charge density, electron energy distribution function and plasma potential in the standard way (Chung *et al.* 1975).

(2c) Neutral Particle Measurements

The concentrations of ground-state and singlet (excited) molecular oxygen are measured by vuv absorption from a continuum source, using the arrangement shown schematically in Fig. 1b. The concentration of atomic oxygen is deduced from the reduction in molecular absorption, and at low concentrations its value derived from the intensity of the OI resonance line emission at 130 nm calibrated against the absorption measurements.

The vuv radiation source is a high-pressure (0.25 bar), krypton filled lamp (Wilkinson and Byram 1965) fitted with a magnesium fluoride output window. Although designed for use in a microwave cavity, best results were obtained when the source was excited by about 10 W of RF power at 7 MHz, capacitively coupled to the lamp via close-fitting foil sleeves, and modulated at 500 Hz. The lamp emits continuum radiation in the range 125–180 nm. The radiation transmitted through the chamber is focussed by a 60 mm focal length magnesium fluoride lens onto the slit of a 0.2 m normal incidence vuv monochromator (Minuteman Model 302-VM) evacuated to below 10^{-5} mbar. The resolution of the monochromator with 30 μm wide slits is about 0.4 nm. The radiation leaving the exit slit is detected by a solar-blind photomultiplier (Type G26E314LF). After pre-amplification and low-pass filtering, the digitised photomultiplier signals (representing the transmitted intensities) are measured using a numerical box-car integration method, taking 15 s for each data point.

We denote the concentration of oxygen molecules inside the chamber in the ground state ($^3\Sigma_g$) and its metastable excited state ($^1\Delta_a$) by $N[\text{O}_2]$ and $N[\text{O}_2^*]$ respectively, and use the subscript p to denote its value when the plasma source is switched 'on'. If $I_0(\lambda)$ is the intensity measured when the chamber is evacuated (i.e. $N[\text{O}_2] = N[\text{O}_2^*] = 0$), and $I(\lambda)$, $I_p(\lambda)$ the signals with the same gas flow but with the plasma source off and on respectively, then we have, without plasma

$$\ln(I_0(\lambda)/I(\lambda)) = N[\text{O}_2]\sigma_x(\lambda)\ell, \quad (1)$$

and with plasma

$$\ln(I_0(\lambda)/I_p(\lambda)) = N_p[\text{O}_2]\sigma_x(\lambda)\ell + N[\text{O}_2^*]\sigma_a(\lambda)\ell, \quad (2)$$

where ℓ is the absorption pathlength, and $\sigma_x(\lambda)$ and $\sigma_a(\lambda)$ are respectively the absorption cross sections for ground state and metastable excited molecules, which are both assumed to be uniformly distributed in the chamber along the beam path of $\ell = 43$ cm.

In practice it is sufficient to measure at only two wavelengths λ_1 , λ_2 , for which (see Table 1) the singlet absorption cross section σ_a is significantly different (Hill 1991), in order to obtain all three quantities $N[\text{O}_2]$, $N_p[\text{O}_2]$ and $N[\text{O}_2^*]$ from the equations above. Confidence in the accuracy of these optical and initial concentration measurements is gained by comparing the cross section for ground state O_2 derived by us at 140 nm, namely $\sigma_x = (1.43 \pm 0.15) \times 10^{-17}$ cm^2 , with the best available

measurement $\sigma_x = (1.42 \pm 0.06) \times 10^{-17} \text{ cm}^2$ (Hill 1991). The mean atomic oxygen density $N[\text{O}]$ is estimated from the reduction in total molecular concentration caused by the discharge, i.e. $N[\text{O}] = 2(N[\text{O}_2] - N_p[\text{O}_2] - N[\text{O}_2^*])$, in which the flow rate is maintained constant and the pumping speed is assumed unchanged.

Table 1. Cross sections at wavelengths used in the absorption measurements

λ (nm)	σ_x (10^{-17} cm^2)	σ_a (10^{-17} cm^2)
140	1.42	0
144	1.40	8.2

(2d) Wool Surface Measurements

To measure the modification of the surface of the wool fibres from hydrophobic to hydrophilic, the specific surface energy difference ΔW for the wool fibres in water was determined using the method described by Hsieh and Yu (1992). This is based on the Wilhelmy (1863) principle and involves measuring the apparent weight change in a rectangular piece of fabric as it is dipped into a liquid, and correcting for the weight of liquid retained in the fabric. A second liquid which fully wets the fibres (zero contact angle) is used to determine the perimeter of the liquid–solid interface in the fabric. Hsieh and Yu (1992) demonstrated that this method of measuring contact angles θ gives the same values as single fibre methods, for a range of materials including cotton. Single fibre measurements for wool were obtained by Brooks and Rahman (1986).

The quantity ΔW is defined as $\Delta W = \gamma_{SV} - \gamma_{SL} = \gamma_{LV} \cos\theta$, where γ_{SV} , γ_{SL} are the specific surface energies J m^{-2} for vapour and liquid covered surfaces respectively, and γ_{LV} is the specific surface energy (surface tension) for the liquid.

Rectangular samples of the fabric were cleaned prior to plasma treatment in accord with a standard solvent extraction method in dichloromethane (IWTO 1966) to remove residual processing lubricants and other possible contaminants. This process has been shown to produce a sufficiently clean surface for X-ray photoelectron spectroscopy analysis of the wool surface (Ward *et al.* 1993). After plasma treatment, samples were stored in sealed containers. Prior to the wettability measurements, the samples were equilibrated under the standard conditions (20°C; 65% relative humidity) used for the measurements.

The chemical state of the wool fibre surface was studied using X-ray photoelectron spectroscopy (XPS). XPS spectra were recorded using a PHI Model 5100 spectrometer, with a Mg $K\alpha$ X-ray source operating at 300 W and with an analyser pass energy of 35 eV. The vacuum pressure in the analyser chamber was always $<10^{-8}$ mbar during analysis with the sample cooled by a liquid nitrogen cold finger. The energy scale was calibrated using the Fermi edge and the Ag $3d_{5/2}$ line (binding energy 367.9 eV), whilst the retardation voltage was calibrated noting the position of the peaks corresponding to Cu $2p_{3/2}$ (binding energy 932.67 eV) and Cu $3p_{3/2}$ (binding energy 75.13 eV).

The wool fibre surfaces were examined in a Hitachi S4100 Field Emission Scanning Electron Microscope (FESEM) operated at a beam energy of 1 keV and beam current at the sample of about 2.5 pA. At this low beam energy, no metal coating of the samples is required.

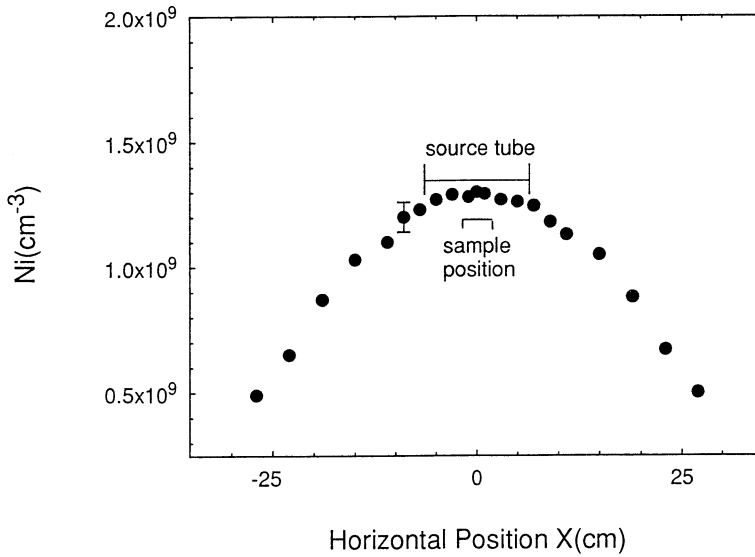


Fig. 2. Spatial profile of ion density along the x axis for $p = 0.03$ mbar and $P = 100$ W. The locations of the plasma source (13 cm diameter) and sample (4 cm) are indicated.

3. Results

The experiments consisted firstly of measuring the concentration of the various plasma constituents in the chamber as functions of RF power P and gas pressure p (in the absence of any wool samples), and secondly the changes, particularly of surface energy, produced in the wool as a function of both plasma conditions and its exposure time in order to relate the changes to the fluxes of appropriate reactive species. The spatial and energy distributions of charged particles could be measured along six horizontal axes of the chamber. The charged-particle density is fairly uniform (Fig. 2) in the region where the sample is located, i.e. at the chamber centre in the plane $y = 0$. The available absorption path restricted measurements of neutral species to a single line-of-sight average. However, since volume atomic recombination and molecular de-excitation can be neglected at the low pressures used, and recombination occurs at the walls with low probability (Sabadil and Pfau 1985; Gousset *et al.* 1989; Donnelly and Rose 1990), about 5% for stainless-steel (Dai 1995), their concentrations can be assumed to be uniform in the chamber. The sample remained close to room temperature during treatment for all the doses used in this study.

It should be noted that during the wool treatment the plasma composition may be slightly modified by the evolution of volatile species from the wool (see Section 3c). While the measured parameters may not be precisely the same as those present at the sample surface during actual treatment, we have assumed this difference to be small.

(3a) Plasma Composition

Fig. 3 shows how the densities of the various plasma components in the chamber (at the sample position) vary with gas pressure at a fixed RF power

(100 W). While the ion density decreases as the pressure is raised, the metastable concentration increases. The atomic oxygen density is greatest around 0.05 mb.

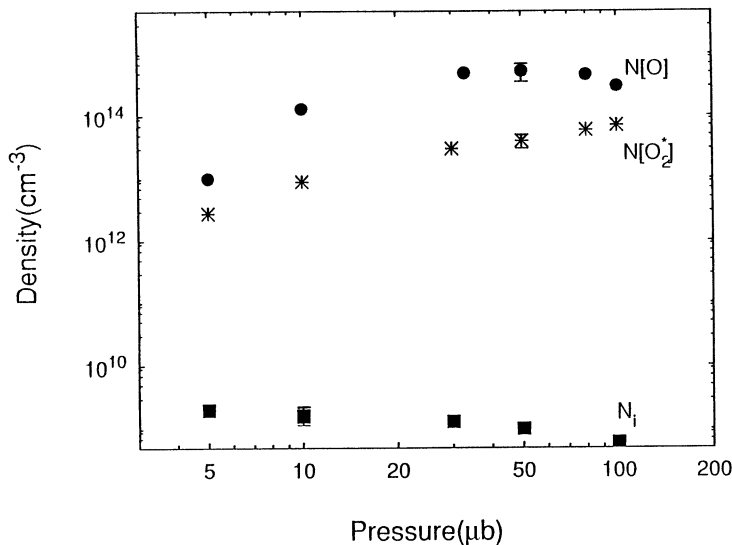


Fig. 3. Concentration of atomic oxygen (solid circles), metastable molecular oxygen (stars) and ions (squares) as functions of pressure at $P = 100$ W.

A typical result is shown in Fig. 4, which plots how the densities of ions $N[\text{O}_2^+]$, metastable oxygen molecules $N[\text{O}_2^*]$, and oxygen atoms $N[\text{O}]$ in the chamber vary with RF power at a fixed pressure of 0.03 mb. The ion density in the reaction chamber increases roughly in proportion to the RF power. While the concentrations of both atomic and metastable molecular oxygen in the reaction chamber increase with RF power up to about 100 W, higher power produces little change. (Atomic oxygen increases somewhat while the metastable molecular density slightly decreases.) The atomic oxygen density is always much higher than that of both the ions and the metastables.

(3b) Changes to Surface Energy of the Wool Fibre

In general, the effect of oxygen plasma treatment is to change the specific surface energy difference from about -4 mJ m^{-2} to as high as $+60 \text{ mJ m}^{-2}$. The measured changes in surface energy ΔW of the fibres as the exposure to oxygen plasma is varied is shown in Figs 5–7: Fig. 5 shows how ΔW varies with the RF power supplied to the source for a fixed time, while Fig. 6 shows the effect of increasing the treatment time at constant RF power (100 W). A rapid approach to saturation (which presumably corresponds to total modification of the fibre surface) is quite evident. The effect of varying the pressure for a given small exposure (corresponding to treatments well below saturation, i.e. at low RF power and short discharge duration) is shown in Fig. 7. Notice that the dependence of ΔW on pressure itself suggests that the effect on the wool is unlikely to be caused by the charged particles, whose density has the opposite trend (Fig. 3).

The most clear-cut relation, and thus one which points to the most likely cause of the observed changes, can be seen by comparing the energy changes ΔW with the total number of oxygen atoms reaching unit area of the surface which is proportional (assuming constant gas temperature) to the product of the atomic oxygen concentration $N[\text{O}]$ and the exposure time t . We find that all the available data can be represented on the single plot shown in Fig. 8,

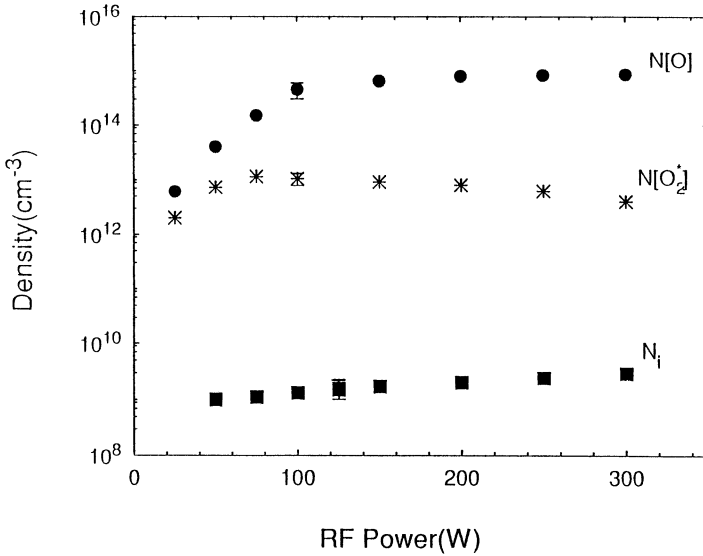


Fig. 4. Concentration of atomic oxygen (solid circles), metastable molecular oxygen (stars) and ions (squares) as functions of RF power at $p = 0.03$ mb.

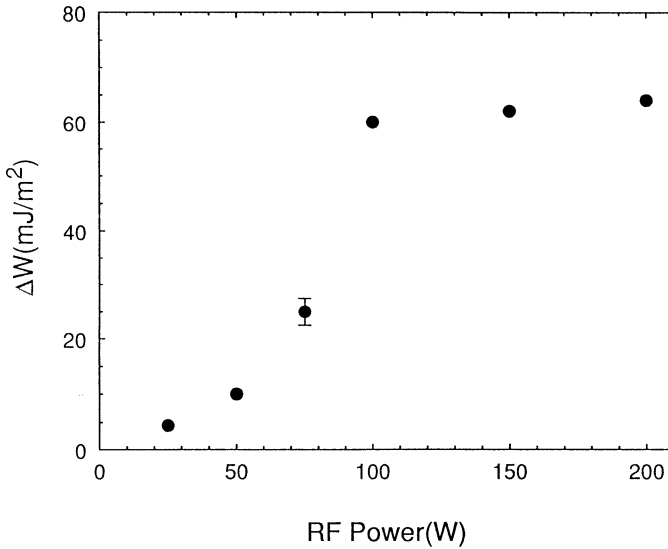


Fig. 5. Dependence on RF power of changes in wool surface energy ΔW at $p = 0.03$ mb and $t = 1$ s.

which includes results for the entire range of discharge conditions examined ($50 \leq P \leq 300$ W, $0.005 \leq p \leq 0.1$ mb or, $0.1 \leq t \leq 600$ s) in oxygen, dry air, as well as argon discharges (the value of $N[O]$ for argon was estimated from the 130 nm resonance line emission). The progressive increase and saturation of the surface energy at an appropriate 'dose' shows a clear correlation with the amount of atomic oxygen reaching the wool.

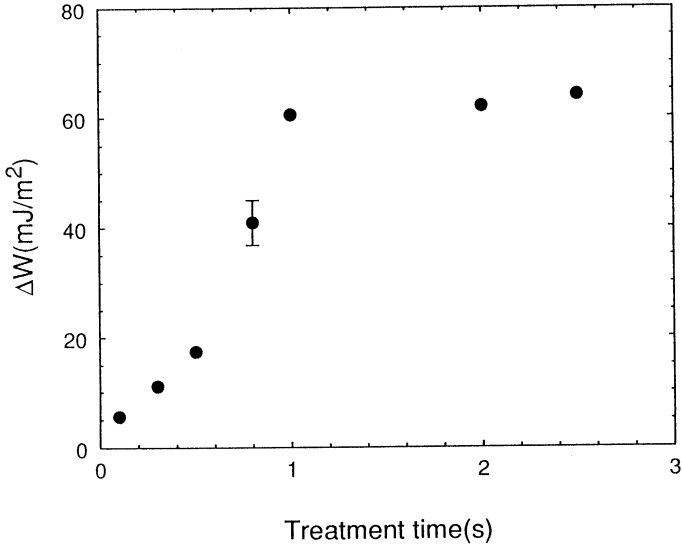


Fig. 6. Effect of treatment time on ΔW at $p = 0.03$ mb and $P = 100$ W.

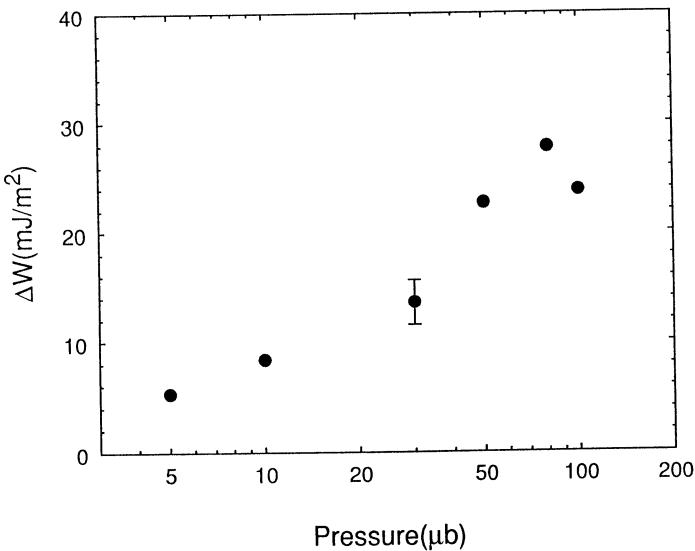


Fig. 7. Dependence of ΔW on pressure at $P = 100$ W and $t = 0.5$ s.

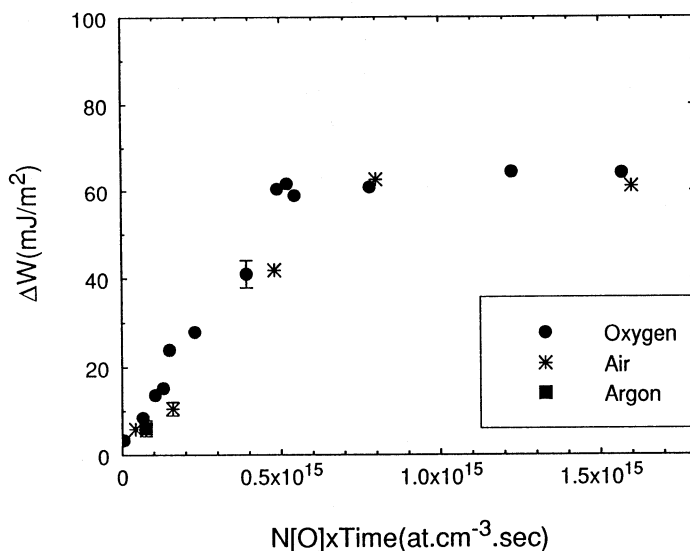


Fig. 8. Dependence of ΔW on the dose of atomic oxygen for all discharge conditions: oxygen, air and Ar.

(3c) Other Studies

Several subsidiary experiments were conducted to help identify the role of plasma constituents other than atomic oxygen. For example, in order to distinguish the effects of charged particles (electrons and ions) from those of reactive neutrals (O , O_2^*), a fine stainless steel wire mesh (with $30 \mu\text{m} \times 30 \mu\text{m}$ holes) was inserted between the source and the reaction chamber. The plasma conditions in the source, typically $N_i \approx 10^{10} \text{ cm}^{-3}$ and $T_e \approx 6 \text{ eV}$, are such that the holes in the mesh were smaller than the local Debye distance ($\lambda_D \approx 200 \mu\text{m}$); thus the mesh considerably reduced the plasma densities in the chamber (to $<10^8 \text{ cm}^{-3}$) while it had only a much smaller effect on the densities of both O and O_2^* (measurements showed them to be reduced respectively by about 30% and 10%). Subsequent measurements on wool samples treated in this way showed that the presence of the mesh led to only a small reduction in ΔW (at a dose roughly half that required to produce saturation).

Table 2. Changes in surface chemical composition measured by XPS for different oxygen plasma conditions

Oxygen plasma conditions	C	Total			Atomic concentration (%)			Sulfur groups	
		O	N	S	C-H; C-C; C=C	Carbon groups C-O; C-O-C	C=O; O-C-O	S-S	SO ₂ ; SO ₃ H
Untreated	70	16	11	3	55	7	8	2.4	0.4
0.03 mb/100 W 0.3 s	69	20	8	2	49	9	12	1.9	0.2
0.01 mb/200 W 60 s	54	28	14	3	30	12	12	1.7	0.9

The significant chemical changes in the surface are shown in Table 2, which shows the effect of increasing levels of oxygen plasma exposure as measured by XPS. The most obvious effect of exposure to oxygen plasma is to noticeably increase the amount of chemically combined oxygen and to decrease that of carbon. There is a clear link between the increasing level of oxidised species present and the changes in surface energy, as shown by comparison of the data in Table 2 and Fig. 8.

The treatments were repeated using discharges in argon, dry air and hydrogen with the results shown in Fig. 9 for two cases using the same power input, treatment time, and gas pressures as for oxygen. They show a very weak effect with argon. On the other hand, a significant effect was observed with air. The absorption spectrum for a discharge in air showed that its oxygen constituent was about 29% dissociated at 0.1 and 46% at 0.03 mb, while the metastable molecular oxygen concentration was too low to measure. Exposure to hydrogen plasma resulted in no measurable change to the surface energy. The chemical changes to the wool surface for these different gases, as revealed by XPS, are summarised in Table 3, and correspond well to the wettability changes. Treatment by argon plasma showed a similar but much weaker effect than oxygen plasma. Treatment by hydrogen plasma showed no observable chemical change.

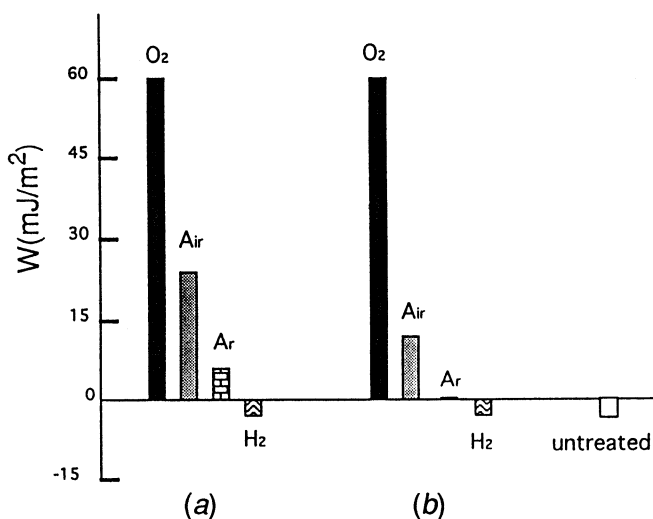


Fig. 9. Effect of different plasma gases on W : (a) $p = 0.1$ mb, $P = 100$ W, $t = 5$ s and (b) $p = 0.03$ mb, $P = 100$ W, $t = 1$ s.

Table 3. Changes in surface chemical composition measured by XPS after extended treatment on different gases (plasma conditions: 0.01 mb/200 W/60 s)

Treatment	Total				Atomic concentration (%)			Sulfur groups	
	C	O	N	S	Carbon groups C-H; C-C; C=C	C-O; C-O-C	C=O; O-C-O	S-S	SO ₂ ; SO ₃ H
Untreated	70	16	11	3	55	7	8	2.4	0.4
H ₂	71	15	11	2	57	7	7	1.7	0.4
Ar	68	20	10	2	51	9	8	1.2	0.3
O ₂	54	28	14	3	30	12	12	1.7	0.9

The vuv emission measurements at the 130 nm OI resonance line showed the presence of atomic oxygen in Ar plasmas. For example, at $p = 0.03$ mb and $P = 200$ W its intensity increased (about three times) when a 225 cm² wool sample was present in the chamber, indicating the release of some volatile oxygenic material (possibly either air or water vapour) from the wool caused by exposure to the plasma.

Images of the untreated and treated wool fibres extracted from fabrics were recorded using the field emission SEM. For the range of treatment conditions reported in this paper, no significant differences were observed. This implies that only the outermost surface layers of the fibres were affected by these treatments.

4. Discussion

All the results obtained and summarised above are evidence that atomic oxygen is the main reactive species responsible for the most significant changes in surface properties, in particular for increasing the surface energy (wettability). This showed not only qualitatively in the general trends with pressure and RF power, but quantitatively through the total exposure to O. The ineffectiveness of the charged particles was clearly demonstrated by the effect of the fine mesh baffle. Similarly, although weak effects can be seen when argon is used, especially with long treatment times, these can also be attributed wholly or partly to the presence of oxygen, either as a background impurity in the gas or vacuum system, or by evolution from the wool itself. This is supported by the observation of OI resonance radiation at 130 nm, as described above.

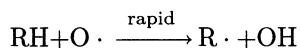
All of these observations are clearly consistent with a model in which the wool surface is modified by plasma as the result of direct gas-surface interactions caused by a single dominant reactive species (atomic oxygen), in which charged particles *per se* play no significant part.

The dominant role of oxygen is seen in the most significant chemical changes shown by the XPS results, i.e. the increase of oxygen at the expense of carbon. It can be shown from reaction rate calculations that under our discharge conditions the main process for producing the active oxygen free radical (O·) is by direct collisional dissociation (Dai 1995):

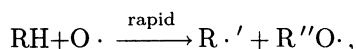


The hydrophobic lipid surface layer consists of long-chain hydrocarbon molecules covalently bound to the underlying protein layers of the fibre cuticle. The model involves attack by the atomic oxygen free radical, whose energy (4.2 eV) is above the bond energies of C-C (3.5 eV) and C-H (4 eV).

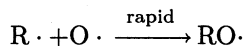
Oxidation is initiated by atomic oxygen radicals by rapid reactions (Hansen and Pascale 1965) of the type



or



where the groups R and R'' denote saturated hydrocarbon chains and R· and R·' alkyl radicals. The alkyl radicals (R·) could then react rapidly with the oxygen radicals:



In this way some new chemical bonds are formed on the wool surface (Table 2), thus rendering the hydrophobic surface hydrophilic. We conclude that the substantial changes in wettability and surface energy resulting from the relatively brief plasma treatments used in this work are due to oxidation by atomic oxygen of the lipid layer which forms the outer surface of the wool fibre. More extensive treatments would be expected to remove this layer and oxidise the underlying protein structures, as has been shown in other studies (Ward *et al.* 1993).

Acknowledgments

The authors are grateful to Dr A. Perry for advice on plasma production and measurements; to Dr B. D. Blackwell for the data acquisition and analysis software; to Dr B. R. Lewis for the loan of the monochromator and his valuable advice on vuv spectroscopy; to Dr P. Turner and Dr B. Holcombe of CSIRO, DWT for their expert advice on wool; to Dr W. Skinner of the South Australian Surface Technology Centre at the University of South Australia for the XPS measurements; and to Mr J. Wach for the design of the apparatus and his expert technical assistance. This research was funded by the Australian Wool Research and Promotion Organization (now International Wool Secretariat).

References

- Brooks, J. H., and Rahman, M. S. (1986). *Textile Res. J.* **56**, 164–71.
- Chou, C-H., Wei, T-C., and Phillip, J. (1992). *J. Appl. Phys.* **72**, 870.
- Chung, P. M., Talbot, L., and Touryan, K. J. (1975). 'Electric Probes in Stationary and Flowing Plasmas: Theory and Application' (Springer: Berlin).
- Crompton, R. W., Hayashi, M., Boyd, D. E., and Makabe, T. (Eds) (1991). 'Gaseous Electronics and Its Applications' (KTK Scientific Publishers: Japan).
- Dai, X. J. (1995). Kinetic model of an rf discharge in oxygen. (in preparation).
- Donnelly, I. J., and Rose, E. K. (1990). *Aust. J. Phys.* **43**, 45.
- Gousset, G., Touzeau, M., Vialle, M., and Ferreira, C. M. (1989). *Plasma Chem. Plasma Processing* **9**, 189.
- Hansen, R. H., and Pascale, J. V. (1965). *J. Polymer Sci. A* **3**, 2205–14.
- Hill, P. C. (1991). Ph.D. Thesis, Australian National University.
- Hsieh, Y-L., and Yu, B. (1992). *Textile Res. J.* **62**, 677–85.
- IWTO Specification of Test Methods (1966). Test IWTO-10-66(E), International Wool Textile Organisation.
- Joubert, O., Pelletier, J., and Arnal, Y. (1989). *J. Appl. Phys.* **65**, 5096.
- Maclaren, J. A., and Milligan, B. (1981). 'Wool Science—the Chemical Reactivity of the Wool Fibre' (Science Press: NSW).
- Rakowski, W. (1989). *Melliand Textiberichte* **70**, 780.
- Sabadil, H., and Pfau, S. (1985). *Plasma Chem. Plasma Processing* **5**, 67.
- Schram, D. C., Bisschops, Th. H. J., Kroesen, G. M. W., and Hoog, F. J. de (1987). *Plasma Phys. Controlled Fusion* **29**, 1353–64.
- Ward, R. J., Willis, H. A., George, G. A., Guise, G. B., Denning, R. J., Evans, D. J., and Short, R. D. (1993). *Textile Res. J.* **63**, 362–8.
- Wilhelmy, J. (1863). *Ann. Physik (Leipzig)* **119**, 177.
- Wilkinson, P. G., and Byram, E. T. (1965). *Appl. Optics* **4**, 581.
- Zawaidah, E., and Kim, N. S. (1988). *J. Appl. Phys.* **64**, 4199.

